

YYDS: Visible-Infrared Person Re-Identification with Coarse Descriptions

Yunhao Du¹, Zhicheng Zhao^{1,2,3}, and Fei Su^{1,2,3}

¹The school of Artificial Intelligence, Beijing University of Posts and Telecommunications

²Beijing Key Laboratory of Network System and Network Culture, Beijing, China

³Key Laboratory of Interactive Technology and Experience System Ministry of Culture and Tourism, Beijing, China
 {dyh_bupt,zhaozc,sufei}@bupt.edu.cn

Abstract. Visible-infrared person re-identification (VI-ReID) is challenging due to considerable cross-modality discrepancies. Existing works mainly focus on learning modality-invariant features while suppressing modality-specific ones. However, retrieving visible images only depends on infrared samples is an extreme problem because of the absence of color information. To this end, we present the **Refer-VI-ReID** settings, which aims to match target visible images from both infrared images and coarse language descriptions (e.g., “a man with red top and black pants”) to complement the missing color information. To address this task, we design a Y-Y-shape decomposition structure, dubbed **YYDS**, to decompose and aggregate texture and color features of targets. Specifically, the text-IoU regularization strategy is firstly presented to facilitate the decomposition training, and a joint relation module is then proposed to infer the aggregation. Furthermore, the cross-modal version of k-reciprocal re-ranking algorithm is investigated, named **CMKR**, in which three neighbor search strategies and one local query expansion method are explored to alleviate the modality bias problem of the near neighbors. We conduct experiments on SYSU-MM01, RegDB and LLCM datasets with our manually annotated descriptions. Both YYDS and CMKR achieve remarkable improvements over SOTA methods on all three datasets. Codes are available at <https://github.com/dyhBUP/YYDS>.

1 Introduction

Person re-identification (ReID) [117] aims to associate person images of the same identities across different cameras and has significant research impacts on intelligent surveillance systems [17, 19]. Benefiting from enormous amount of annotated data, deep learning based methods have achieved impressive success in recent years [34, 35, 57, 58, 69, 88, 133, 139, 140]. However, their practical application is limited since only visible (RGB) modality is considered, which loses efficacy under low-light condition.

To meet the need for 24-hour surveillance systems, visible-infrared person re-identification (VI-ReID) is attracting increasing attentions. Instead of performing matching within the visible modality, VI-ReID aims to retrieve visible targets

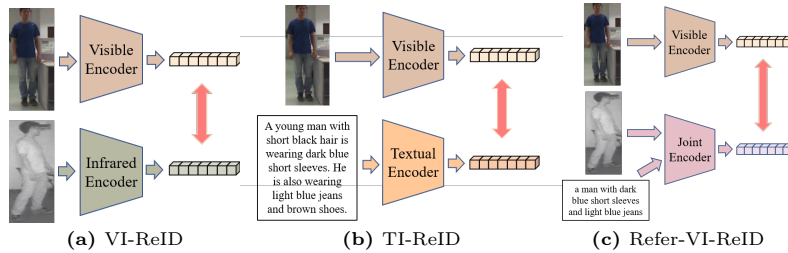


Fig. 1: Comparison between different task settings. (a) Visible-Infrared ReID. (b) Text-Image ReID. (c) Our proposed referring visible-infrared ReID.

with infrared probes [16, 61, 101]. Most existing VI-ReID methods perform *shared feature learning*, which focus on embedding the features from different modalities into the same feature space [7, 14, 23, 64, 93, 111–113, 116, 119]. Nevertheless, modality-specific information in both visible and infrared modalities are abandoned, including some discriminative details. Differently, *feature compensation learning* methods try to make up the missing modality-specific cues from one modality to another [39, 91, 97, 126, 136]. However, it is an ill-posed problem to fill in the missing information in modality, e.g., color cues. This issue prompts us to consider a more sound strategy for information compensation.

Text-image person re-identification (TI-ReID) is one of the current research hotspots due to its wide application and flexibility [45, 56, 73, 85, 95, 105, 125, 135]. It can search for the target pedestrian by the witness’s language descriptions when visible probes are not available. The success of TI-ReID proves that textual descriptions can provide discriminative information for person retrieval. Inspired by this, we propose referring visible-infrared person re-identification (**Refer-VI-ReID**) settings, which uses coarse descriptions, e.g., “a man with dark blue short sleeves and light blue jeans”, to assist infrared images in retrieving visible images. Fig. 1 illustrates the difference between VI-ReID, TI-ReID and Refer-VI-ReID.

The main challenge of Refer-VI-ReID lies in the misalignment between query modality (infrared and text) and gallery modality (visible). The effectiveness of two-stream frameworks has been verified in previous cross-modal works [13, 18, 38, 70, 96]. In this paper, we extend this pipeline by designing a Y-Y-shape decomposition structure (**YYDS**) in the spirit of *divide and conquer*, as shown in Fig. 2. Specifically, it includes two symmetric Y-shape branches to disentangle texture and color features from query and gallery samples respectively. Previous disentanglement learning works tend to utilize auto-encoders [51] or GANs (Generative Adversarial Networks) [27] to separate ID-discriminative factors and ID-excluded factors [9, 26, 59, 130, 134], which suffer from difficult convergence and high training cost. Some other works use extra clues (e.g., attributes, segmentation) to force the model to focus on identity information [6, 22], and don’t take full advantage of the complementary features. Differently, our Y-shape branch applies two separate encoders to extract complementary texture and color features individually. Afterwards, they are dynamically aggregated by a joint encoder

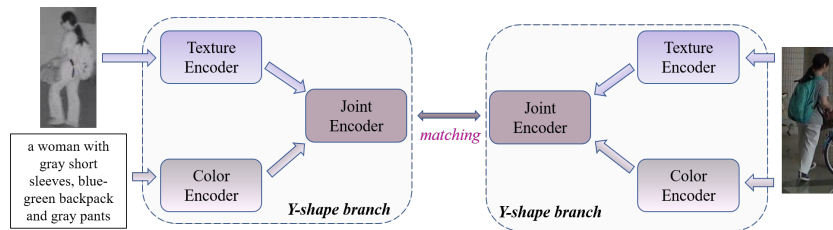


Fig. 2: Overview of our Y-Y-shape decomposition structure.

with asymmetric relation operation to predict the output features. While training, texture and joint encoders are optimized with common ReID loss, and color encoders are optimized by Kullback-Leibler divergence loss with novel text-IoU regularization. This design helps the network to extract both discriminative and complete representations without requiring adversarial or generative training.

K -reciprocal re-ranking [137] is widely used to revise the initial ranking list [16, 47, 63, 68, 89, 92, 94]. It first searches for k -reciprocal nearest neighbors for each sample, and then embeds them into k -reciprocal features to calculate the Jaccard distance for re-ranking. This strategy stands out from other re-ranking methods [74, 86, 129] with its superior performance and unsupervised manner. However, we find that it only brings limited performance improvements when applied to cross-modal tasks, e.g., VI-ReID. Specifically, it is observed that neighbors are dominated by intra-modal samples (including many negative samples), while few cross-modal positive samples are included. We refer to this problem as *neighbor modality bias*, which is caused by the difference in intra-modal and inter-modal distance distributions. Some previous works try to alleviate it by constraining the search domain of neighbors to the gallery set, which helps exclude intra-modal negative samples [24, 44, 60]. However, we find this *constrained* strategy to be suboptimal because rich intra-modal context information is discarded. To crack this nut, we propose two novel strategies, *divided* and *extended*, to introduce cross-modal positive neighbors while retaining intra-modal neighbors. Furthermore, a modality-aware local query expansion (MA-LQE) strategy is designed to enhance the robustness of neighbor features. Experiments demonstrate the superiority of our proposed method, dubbed (CMKR).

The main contributions can be summarized as follows:

- We introduce the Refer-VI-ReID task setting, which assists visible-infrared retrieval with complementary textual information.
- We propose YYDS to perform texture and color feature disentanglement and aggregation to output discriminative and complete features.
- We design the CMKR algorithm, which extends k -reciprocal re-ranking to cross-modal scenarios and mitigates the effect of neighbor modality bias.
- Extensive experiments are conducted on SYSU-MM01, RegDB and LLCM to demonstrate the effectiveness of our methods.

2 Related Work

2.1 Visible-Infrared Person ReID

Visible-infrared person ReID is challenging due to the cross-modality discrepancies between visible and infrared images. Metric learning is widely used to narrow the gap between the two modalities by elaborately designing objective functions, such as bi-directional dual-constrained top-ranking (BDTR) loss [113, 119], hetero-center triplet loss [64], Margin MMD-ID loss [41], and so on [31, 32, 37, 62, 108, 112, 141]. Some other works focus on the network structure, e.g., partially shared two-stream framework [30, 110], neural search based methods [7, 23], adaptive style normalization [102], attention-based methods [46, 75, 98], etc. Differently, generation-based methods utilize generative models [27, 49, 51] to produce auxiliary samples [20, 39, 50, 54, 79, 90, 91, 99, 128, 131] or medial features [120, 126], or to realize disentanglement learning [10, 78, 123]. Though their effectiveness, these methods suffer from high computational cost and difficult convergence while training. Inspired by this, another series of works directly utilize data augmentation [15, 40, 48, 102, 115] or image transformation [2, 55, 65, 118, 122] strategies to generate diverse samples.

Recently, several works alleviate the cross-modal issues by introducing extra clues to learn discriminative representations. Zhang *et al.* [124] manually annotated attribute labels as auxiliary information to train the model with attribute classification losses. Zheng *et al.* [132] further designed a progressive attribute embedding strategy to effectively fuse attribute information and visual information. Chen *et al.* [5] proposed to utilize key points to dynamically select discriminative appearance regions. Feng *et al.* [22] decorrelated modality-shared features into shape-related and shape-erased features under the guidance of human parsing maps. Different from previous works, we present a novel Y-Y-shape structure to assist cross-modal retrieval with coarse descriptions, which yields a wider range of applications.

2.2 Re-ranking

Re-ranking is commonly used in various retrieval tasks, which aims to revise the initial ranking list with sample-to-sample similarity. Jegou *et al.* [42, 43] presented an iterative approach to reduce the neighborhood non-reversibility rate. Qin *et al.* [81] formally defined the concept of k -reciprocal nearest neighbors, and utilized two rounds of query expansion to circumvent the non-reciprocity of near neighbor relationships. Leng *et al.* [52, 53] proposed the bi-directional ranking mechanism and considered both content and context similarity. Similarity, García *et al.* [25] applied content and context information to remove the visual ambiguity. Ye *et al.* [109, 114] pursued accurate retrieval results by aggregating multiple ranking lists. Bai *et al.* [1] designed an elaborate pipeline called the sparse contextual activation (SCA), which measures the dissimilarity between samples by the Jaccard distance of neighbor features. Zhong *et al.* [137] extended from SCA by integrating the idea of k -reciprocal nearest neighbors. Yu

et al. [121] exploited the diversity of high-dimensional features in the spirit of “divide and fuse”. Sarfraz *et al.* [84] directly calculated the averaged distance of expanded neighbors as the final measurement. Guo *et al.* [29] introduced a soft version of k -reciprocal nearest neighbors with a density-adaptive kernel technique. Peng *et al.* [77] assumed that the probe image and its neighbors lie in a locally linear manifold and obtained neighbor features with linear reconstruction. Chen *et al.* [8] improved Jaccard distance in an camera-aware manner.

These re-ranking methods have shown significantly improved performance in single-modal retrieval tasks. Nevertheless, limited performance is observed when directly applying them to cross-modal scenarios caused by the neighbor modality bias problem. Existing methods [24, 44, 60] tackled this problem by searching neighbors only in the gallery set. We argue that this “constrained” strategy is suboptimal because it ignores substantial context information in the query set. In this paper, we propose a novel cross-modal k -reciprocal re-ranking algorithm to avoid such a dilemma.

3 Method

3.1 Preliminary

Let us take $\mathcal{X}^v = \{x_n^v\}_{n=1}^{N^v}$ and $\mathcal{X}^i = \{x_n^i\}_{n=1}^{N^i}$ to denote visible and infrared images, where x_n^v and x_n^i are images, and N^v and N^i are the number of visible and infrared images. The corresponding identity labels are defined as $\mathcal{Y}^v = \{y_n^v\}_{n=1}^{N^v}$ and $\mathcal{Y}^i = \{y_n^i\}_{n=1}^{N^i}$. Coarse descriptions $\mathcal{X}^t = \{x_n^t\}_{n=1}^{N^t}$ are manually annotated for each infrared image, where samples of the same identity share the same description. The goal of Refer-VI-ReID is to match samples across modalities by learning modality invariant representations $\mathcal{F}^v = \{f_n^v\}_{n=1}^{N^v}$ and $\mathcal{F}^i = \{f_n^i\}_{n=1}^{N^i}$. While inference, given a pair of query infrared image and coarse description $q = \{q^i, q^t\} \in \mathcal{Q}$, the retrieval ranking list $\mathcal{RL}(q) = \{g_1^v, g_2^v, \dots, g_{N_g}^v | g_n^v \in \mathcal{G}\}$ is generated according their feature similarities with the visible gallery set \mathcal{G} .

3.2 YYDS

3.2.1 Overview

It is assumed that the identity discriminative features in visible person images include color features and texture features. However, infrared images only contain texture information and lack sufficient color information. Inspired by this, we propose to utilize language descriptions to complete the missing color information with a novel color-texture disentanglement framework. Fig.3 (left) illustrates the designed Y-Y-shape decomposition structure (YYDS), which primarily comprises two branches, i.e., visible Y-shape branch and infrared Y-shape branch. The two branches share the similar structure, including a color encoder E_c^* , a texture encoder E_t^* and a joint relation module (JRM) E_j^* , where $*$ \in v, i represents image modalities.

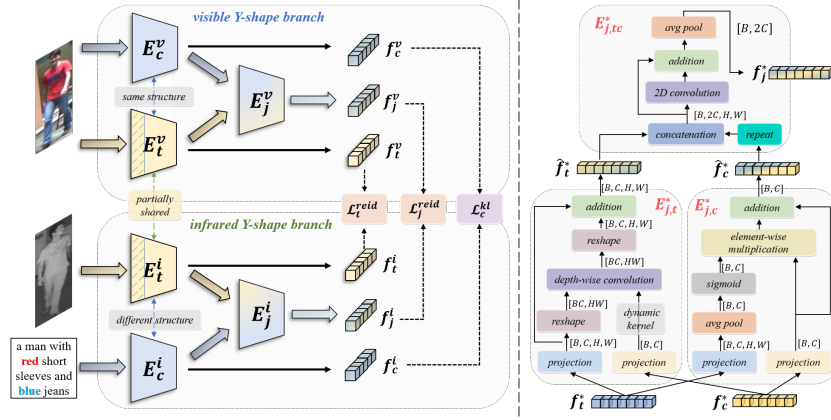


Fig. 3: **Left:** The framework of YYDS, which includes a visible Y-shape branch and an infrared Y-shape branch. Each branch consists of a color encoder E_c^* , a texture encoder E_t^* and a joint relation module (JRM) E_j^* . The two E_t^* partially share weights to eliminate modality-specific information. During training, the overall framework is optimized by two ReID loss \mathcal{L}_t^{reid} , \mathcal{L}_j^{reid} and one KL divergence loss \mathcal{L}_c^{kl} with text-IoU regularization. **Right:** The details of JRM, which is composed of texture-centered relation block $E_{j,t}^*$, color-centered relation block $E_{j,c}^*$ and joint relation block $E_{j,tc}^*$. B is the batch size, C is the channel dimension, and H, W is the size of feature map.

Specifically, it takes a mini-batch of triplets $\{x_n^v, x_n^i, x_n^t\}_{n=1}^{N_B}$ as inputs, where N_B is the batch size. For simplification, the subscript n is omitted in the following descriptions. The two texture encoders E_t^v and E_t^i are utilized to extract texture embeddings $f_t^* = E_t^*(x^*)$, $*$ $\in \{v, i\}$, which utilizes ResNet-50 [33] as the backbone and the last stride is set to 1. Following previous VI-ReID works [30, 110], the first convolutional blocks in E_t^v and E_t^i don't share weights to capture modality-specific low-level features, and the parameters of deeper blocks are shared to learn high-level texture features. As for color encoders, the E_c^v share the same structure with E_t^v with unshared parameters to capture color features from visible images $f_c^v = E_c^v(x^v)$. Differently, E_c^i takes descriptions x^t as input $f_c^i = E_c^i(x^t)$, which applies RoBERTa [66] as the backbone. Afterwards, joint relation modules E_j^* , $*$ $\in \{v, i\}$ are designed to dynamically aggregate the decomposed color embeddings f_c^* and f_t^* , and output the joint embeddings $f_j^* = E_j^*(f_c^*, f_t^*)$ (details in Sec 3.2.2).

During training, the three pairs of encoders $\{E_c^v, E_c^i\}$, $\{E_t^v, E_t^i\}$ and $\{E_j^v, E_j^i\}$ are optimized by one Kullback-Leibler (KL) divergence loss \mathcal{L}_c^{kl} and two common ReID losses \mathcal{L}_t^{reid} and \mathcal{L}_j^{reid} respectively (details in Sec 3.2.3). While inference, the triplet of embeddings $\{f_c^*, f_t^*, f_j^*\}$ are concatenated along the channel dimension to obtain the final features f^* , $*$ $\in \{v, i\}$.

3.2.2 Joint Relation Module

The details of joint relation modules (JRM) E_j^* are shown in Fig.3 (right), which consists of three relation blocks $E_{j,t}^*$, $E_{j,c}^*$ and $E_{j,tc}^*$. The motivation is to first perform mutual modulation between color and texture embeddings f_c^* and f_t^* with color-centered relation block $E_{j,c}^*$ and texture-centered relation block $E_{j,t}^*$, and then the two modulated features are aggregated with the joint relation block $E_{j,tc}^*$.

Because of the great discrepancy between f_c^* and f_t^* , the mutual modulation procedure is designed in an asymmetric manner, i.e., *channel-level modulation* and *spatial-level modulation*. For $E_{j,c}^*$, f_c^* and f_t^* are first embedded by two projection heads. Then, the channel modulation weights w_t^* are generated by projected texture features \bar{f}_t^* with an average pooling layer and a sigmoid layer:

$$w_t^* = \text{sigmoid}(\text{pool}(\bar{f}_t^*)). \quad (1)$$

Then the projected color features \bar{f}_c^* is modulated by multiplying w_t^* with a residual addition:

$$\hat{f}_c^* = w_t^* \times \bar{f}_c^* + \bar{f}_c^*, \quad (2)$$

where \times denotes element-wise multiplication. As to $E_{j,t}^*$, f_c^* and f_t^* are also passed through two projection heads firstly to output \tilde{f}_c^* and \tilde{f}_t^* . Different from f_c^* , the texture features f_t^* contain rich spatial contextual clues. Inspired by this, the dynamic convolution is performed to modulate local spatial features in \tilde{f}_t^* under the guidance of \tilde{f}_c^* . Specifically, we take \tilde{f}_c^* as dynamic kernels to convolute with \tilde{f}_t^* by depth-wise convolution [11, 36, 87]. Then a residual addition is followed for optimization stability:

$$\hat{f}_t^* = DWConv(\tilde{f}_t^*; \tilde{f}_c^*) + \tilde{f}_t^*, \quad (3)$$

where $DWConv(\cdot; \cdot)$ represents depth-wise convolution.

After obtaining modulated features \hat{f}_c^* and \hat{f}_t^* , the joint relation block $E_{j,tc}^*$ is introduced to conduct aggregation. \hat{f}_c^* is first repeated in spatial dimensions and then is concatenated with \hat{f}_t^* along the channel dimension to output \hat{f}_{tc}^* . Afterwards, a 2D convolution layer with residual addition and an average pooling layer are utilized to extract the joint embeddings f_j^* :

$$f_j^* = \text{pool}(\text{conv}(\hat{f}_{tc}^*) + \hat{f}_{tc}^*). \quad (4)$$

In conclusion, the two disentangled embeddings f_c^* and f_t^* are first modulated by each other in channel and spatial dimensions respectively, and then are aggregated to output the final discriminative and complete embeddings f_j^* .

3.2.3 Training Loss

Commonly used ReID losses (cross-entropy loss and triplet loss) \mathcal{L}_t^{reid} and \mathcal{L}_j^{reid} are utilized to train texture encoders E_t^* and JRM E_j^* respectively. Please note that our framework can adapt to various VI-ReID backbones and losses. In



Fig. 4: The illustration of text-IoU regularization. Only x_1 shares the same identity with x_0 , but x_2 and x_3 share similar color clues with x_0 .

this paper, we take DEEN [127] as baseline, and their proposed CPM loss and orthogonal loss are also included in our ReID losses.

As to color encoders, the distribution matching loss based on Kullback-Leibler (KL) divergence is applied as in previous text-image ReID works [45, 125]:

$$\mathcal{L}_c^{kl} = \frac{1}{N_B} \sum_{n=1}^{N_B} \sum_{m=1}^{N_B} p_{n,m} \log\left(\frac{p_{n,m}}{q_{n,m} + \epsilon}\right), \quad (5)$$

where $p_{n,m}$ is the probability of matching pairs $\{f_n, f_m\}$, $q_{n,m}$ is the true matching probability, and $\epsilon = 1e^{-8}$ is applied to avoid numerical problems. In implementation, four pairs of features are used to calculate the KL loss, i.e., $\{f_c^v, f_c^i\}$, $\{f_c^i, f_c^v\}$, $\{f_c^v, f_c^v\}$ and $\{f_c^i, f_c^i\}$.

However, different identities may share similar color information. Fig.4 illustrates an example, where x_0 has the same identity only with x_1 , but are also dressed in similar colors with x_2 and x_3 . The color encoders would be confused while being optimized by true matching probability $q_{0,*} = [1, 0, 0, 0, 0]$ as in Eq.5. To circumvent such issue, we propose a text-IoU regularization strategy, which replace the original $q_{n,m}$ with text-IoU based probability $\hat{q}_{n,m}$. Concretely, given a description x_n^t , NLTK [3] is utilized to extract color words $c_n = \{w_1, \dots, w_{N_n}\}$. Then, the text-IoU between samples n and m is defined by the intersection over union of their color word sets:

$$IoU_{n,m} = \frac{|c_n \cap c_m|}{|c_n \cup c_m|}, \quad (6)$$

where $|\cdot|$ is the cardinality of sets. Finally, the normalized text-IoU is utilized as the regularization probability $\hat{q}_{n,m}$ to replace $q_{n,m}$ in Eq.5, which equals to $[0.4, 0.4, 0.2, 0, 0]$ in the example in Fig.5.

Overall, the objective function of our YYDS can be summarized as follows:

$$\mathcal{L}_{total} = \lambda_t \mathcal{L}_t^{reid} + \lambda_j \mathcal{L}_j^{reid} + \lambda_c \mathcal{L}_c^{kl}. \quad (7)$$

3.3 CMKR

3.3.1 Overview

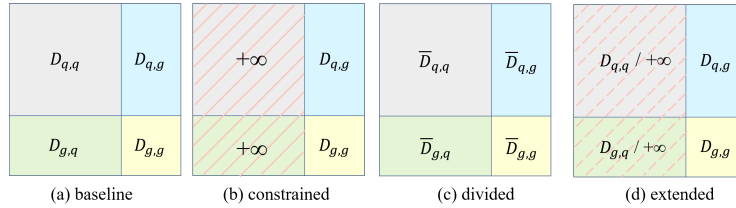


Fig. 5: The illustration of different neighbor strategies from the perspective of distance matrices. (a) The baseline method searches for neighbors based on the original distance matrix. (b) The constrained strategy limits the search domain to the gallery set. (c) The divided strategy separately normalizes the four submatrices. (d) The extended strategy integrates the baseline and constrained strategies.

The k -reciprocal re-ranking algorithm [137] is widely utilized to refine the initial ranking list in the testing stage. Given N_q query images and N_g gallery images, the original distance matrix $D_{ori} \in \mathbb{R}^{(N_q+N_g) \times (N_q+N_g)}$ can be represented as the concatenation of four submatrices:

$$D_{ori} = \begin{bmatrix} D_{q,q} & D_{q,g} \\ D_{g,q} & D_{g,g} \end{bmatrix}, \quad (8)$$

where $D_{q,q} \in \mathbb{R}^{N_q \times N_q}$ is the distance between all query images, and the others are similar. The k -reciprocal nearest neighbors of query q_i are defined as:

$$R(q_i, k_1) = \{g_j | (g_j \in N(q_i, k_1)) \wedge (q_i \in N(g_j, k_1))\}, \quad (9)$$

where $N(q_i, k_1)$ is the k -nearest neighbors of q_i searched based on D_{ori} . For ease of calculation, $R(q_i, k_1)$ is transformed to neighbor features $V_i \in \mathbb{R}^{(N_q+N_g)}$, which is further refined by the local query expansion (LQE) strategy [12, 28, 82]:

$$\tilde{V}_i = \frac{1}{k_2} \sum_{q_j \in N(q_i, k_2)} V_j. \quad (10)$$

Finally, the Jaccard distance based on refined neighbor features are calculated to perform re-ranking:

$$d_{Jacc}(q_i, g_j) = 1 - \frac{\sum_{n=1}^{N_q+N_g} \min(\tilde{V}_{i,n}, \tilde{V}_{j,n})}{\sum_{n=1}^{N_q+N_g} \max(\tilde{V}_{i,n}, \tilde{V}_{j,n})}, \quad (11)$$

where $\tilde{V}_{i,n}$ is the n -th element of \tilde{V}_i .

3.3.2 Neighbor Strategy

The performance of re-ranking is greatly affected by the accuracy of searched neighbors. However, in cross-modal scenarios, neighbors tend to be dominated by intra-modal positive and negative samples, including very few cross-modal

samples. To solve this neighbor modality bias problem, we study three neighbor strategies, i.e., *constrained*, *divided* and *extended* strategies.

Constrained. An intuitive solution is to constrain the neighbor search domain, as done in [24, 44, 60]. Specifically, define $N_{q \rightarrow g}(q_i, k_1)$ as the cross-modal neighbors of q_i among gallery sets, and the constrained neighbors $R_{q \rightarrow g}$ is:

$$R_{q \rightarrow g}(q_i, k_1) = \{g_j | (g_j \in N_{q \rightarrow g}(q_i, k_1)) \wedge (q_i \in N_{g \rightarrow q}(g_j, k_1))\}, \quad (12)$$

which is utilized to replace the original neighbors $R(q_i, k_1)$ in Eq.9. However, we argue that this strategy is suboptimal because it retains cross-modal samples at the expense of losing intra-modal contextual information, which is solved by the following two strategies.

Divided. The neighbor modality bias problem is mainly caused by the distribution inconsistency between intra-modal distances $D_{q,q}/D_{g,g}$ and cross-modal distances $D_{q,g}/D_{g,q}$. Inspired by this, the divided strategy conducts row min-max normalization to these four submatrices separately, and then concatenates them into a new distance matrix:

$$D_{div} = \begin{bmatrix} \bar{D}_{q,q} & \bar{D}_{q,g} \\ \bar{D}_{g,q} & \bar{D}_{g,g} \end{bmatrix}, \quad (13)$$

where $\bar{D}_{*,*}$ is the row-normalized $D_{*,*}$. Then, D_{div} is applied to replace D_{ori} in Eq.8 for neighbor search.

Extended. Different from the *divided* strategy which operates on the distance matrix, the extended directly extends the original neighbor set by introducing cross-modal neighbors. Specifically, it takes the union of $R(q_i, k_1)$ in Eq.9 and $R_{q \rightarrow g}(q_i, k_1)$ in Eq.12 as the final neighbor set:

$$R_{ext}(q_i, k_1) = R(q_i, k_1) \cup R_{q \rightarrow g}(q_i, k_1), \quad (14)$$

which is used to calculate the neighbor features.

Fig.5 illustrates the comparison between baseline and the three proposed neighbor strategies from the perspective of distance matrices. Experiments will demonstrate the superiority of the proposed neighbor strategies over the baseline method.

3.3.3 MA-LQE

The refined neighbor features \tilde{V}_i in Eq.10 also suffer from the neighbor modality bias problem, because $N(q_i, k_2)$ is mainly composed of intra-modal samples. To alleviate this issue, we propose modality-aware local query expansion (MA-LQE) method, which searches for intra-modal and inter-modal neighbors separately to refine the neighbor features:

$$\hat{V}_i = \frac{1}{k_2} \sum_{q_j \in \hat{N}(q_i, k_2, k_3)} V_j, \quad (15)$$

where $\hat{N}(q_i, k_2, k_3) = N_{q \rightarrow q}(q_i, k_2 - k_3) \cap N_{q \rightarrow g}(q_i, k_3)$ explicitly integrates $(k_2 - k_3)$ intra-modal neighbors and k_3 cross-modal neighbors.

Table 1: Comparison with the state-of-the-art VI-ReID methods on SUSY-MM01 under the single-shot protocol. “Epoch” represents the training epochs.

Method	Reference	Epoch	All Search				Indoor Search			
			R-1	R-10	R-20	mAP	R-1	R-10	R-20	mAP
cmGAN [14]	IJCAI2018	2000	26.97	67.51	80.56	27.80	31.63	77.23	89.18	42.19
AlignGAN [91]	ICCV2019	250	42.40	85.00	93.70	40.70	45.90	87.60	94.40	54.30
MHM [106]	AAAI2020	30	35.90	73.00	86.10	38.00	-	-	-	-
JSIA [90]	AAAI2020	650	38.10	80.70	89.90	36.90	43.80	86.20	94.20	52.90
XIV [54]	AAAI2020	120	49.92	89.79	95.96	50.73	-	-	-	-
DDAG [116]	ECCV2020	80	54.75	90.39	95.81	53.02	61.02	94.08	98.41	67.98
LbA [75]	ICCV2021	80	55.41	-	-	54.14	58.46	-	-	66.33
CM-NAS [23]	ICCV2021	120	61.99	92.87	97.25	60.02	67.01	97.02	99.32	72.95
CAJ [115]	ICCV2021	100	69.88	95.71	98.46	66.89	76.26	97.88	99.49	80.37
MPANet [104]	CVPR2021	140	70.58	96.21	98.80	68.24	76.74	98.21	99.57	80.95
SFANet [65]	TNNLS2021	80	65.74	92.98	97.05	60.83	71.60	96.60	99.45	80.05
MSCLNet [126]	ECCV2022	200	76.99	97.63	99.18	71.64	78.49	99.32	99.91	81.17
PAENet [132]	MM2022	80	74.22	99.03	99.97	73.90	78.04	99.58	100.00	83.54
DEEN [127]	CVPR2023	150	74.70	97.60	99.20	71.80	80.30	99.00	99.80	83.30
CAL [103]	ICCV2023	100	74.66	96.47	-	71.73	79.69	98.93	-	83.68
SAAI [21]	ICCV2023	160	75.90	-	-	77.03	83.20	-	-	88.01
MUM [120]	ICCV2023	90	76.24	97.84	-	73.81	79.42	98.09	-	82.06
DARD [100]	TIFS2023	300	69.33	94.32	97.52	65.65	77.21	98.32	99.18	81.91
TransVI [4]	TCSVT2023	80	71.36	96.77	98.26	68.63	77.40	98.69	99.82	81.31
TMD [67]	TMM2023	80	73.92	96.29	98.76	67.76	81.16	98.87	99.68	78.88
STAR [102]	TMM2023	100	76.07	97.76	-	72.73	83.47	99.04	-	85.76
Baseline	ours	80	72.36	96.56	99.03	68.24	78.50	98.45	99.50	82.06
YYDS	ours	80	85.54	99.30	99.78	81.64	89.13	99.66	99.96	91.00
YYDS+CMKR	ours	80	95.51	99.68	99.80	93.77	98.59	99.64	100.00	98.41

Table 2: Comparison with the state-of-the-art VI-ReID methods on harsh lighting datasets RegDB and LLCM under the infrared-to-visible protocol.

Method	Reference	RegDB				LLCM			
		R-1	R-10	R-20	mAP	R-1	R-10	R-20	mAP
DDAG [116]	ECCV2020	68.1	85.2	90.3	61.8	41.0	73.4	81.9	49.6
LbA [75]	ICCV2021	67.5	-	-	72.4	44.6	78.2	86.8	53.8
AGW [117]	TPAMI2021	-	-	-	-	46.4	77.8	85.2	54.8
CAJ [115]	ICCV2021	84.8	95.3	97.5	77.8	48.8	79.5	85.3	56.6
DART [107]	CVPR2022	82.0	-	-	73.8	52.2	80.7	87.0	59.8
MMN [128]	MM2021	87.5	96.0	98.1	80.5	52.5	81.6	88.4	58.9
DEEN [127]	CVPR2023	89.5	96.8	98.4	83.4	54.9	84.9	90.9	62.9
Baseline	ours	89.1	96.8	98.5	81.8	56.5	85.3	91.3	63.2
YYDS	ours	90.2	97.3	98.8	83.5	58.2	87.2	92.6	65.1
YYDS+CMKR	ours	96.6	98.9	99.6	96.1	73.4	91.3	94.6	77.4

4 Experiments

4.1 Datasets and Evaluation Protocol

SYSU-MM01 [101] is the first large-scale benchmark dataset for VI-ReID, which is collected by 4 visible and 2 infrared cameras in both indoor and outdoor environments. The training set contains 395 identities, including 22,258 visible images and 11,909 infrared images. The test set contains 96 identities, with 3,803 infrared images for query and 301/3010 (single-shot / multi-shot) randomly selected visible images as the gallery set. Meanwhile, it contains two test modes, i.e., all-search and indoor-search modes.

RegDB [72] is a harsh lighting dataset, which is collected by a dual-camera system. There are 206 identities for training and 206 identities for testing. Each person has 10 visible images and 10 infrared images. It contains two test modes, i.e., visible-to-infrared and infrared-to-visible modes.

LLCM [127] is a recently proposed low-light VI-ReID dataset, which is collected by 9 cameras in low-light environments. The training set contains 30,921 images of 713 identities, and the test set contains 13,909 images of 351 identities. Both visible-to-infrared and infrared-to-visible modes are used for evaluation.

Evaluation Protocol. We evaluate our model on the 10 trials with different training/testing splits to achieve stable performance following previous works [116, 127]. The cumulative matching characteristics (CMC) [71] and mean average precision (mAP) are adopted as evaluation metrics.

4.2 Implementation Details

YYDS. We implement YYDS with PyTorch [76] on 2 NVIDIA Tesla T4 GPUs. While training, each training mini-batch consists of 4 identities, and each identity contains 4 visible images and 4 infrared images. We utilize DEEN [127] with pretrained ResNet-50 [33] on ImageNet [83] as baseline. All input images are resized to $3 \times 384 \times 144$, and several data augmentation techniques are adopted, i.e., random gray scale, random cropping, random horizontal flipping and random erasing [138]. The overall framework is trained for 80 epochs by SGD optimizer with momentum parameter $p=0.9$ [80]. The learning rate gradually rises up to $\eta=0.1$ by the warm-up scheme for the first 10 epochs, and decays by a factor of 10 at the 20th and 50th epochs. The hyper-parameters in Eq.7 λ_t , λ_j and λ_c are set to 1, 1 and 1.

CMKR. While testing, the Jaccard distance d_{Jacc} is combined with original feature distance to perform re-ranking with a weight λ_{Jacc} . For fair comparison, the best hyper-parameters are selected for each neighbor strategy respectively by grid search.

4.3 Comparison with State-of-the-art Methods

We compare the proposed ‘‘YYDS+CMKR’’ with the state-of-the-art VI-ReID methods on one excellent lighting dataset SYSU-MM01 and two harsh lighting

Table 3: Ablation study on different components of YYDS on SYSU-MM01. **Baseline:** Only texture encoders are utilized. **Color:** Both texture and color encoders are adopted. **IoU:** Text-IoU regularization is used. **Joint:** All three encoders are used.

Method	Color	IoU	Joint	R-1	R-10	R-20	mAP
Baseline	-	-	-	72.36	96.56	99.03	68.24
	✓	-	-	83.66 (+11.30)	99.22 (+2.66)	99.83 (+0.80)	78.90 (+10.66)
	✓	✓	-	84.54 (+12.18)	98.84 (+2.28)	99.63 (+0.60)	80.01 (+11.77)
	✓	✓	✓	85.54 (+13.18)	99.30 (+2.74)	99.78 (+0.75)	81.64 (+13.40)

Table 4: Ablation study on different components of JRM on SYSU-MM01.

Method	R-1	R-10	R-20	mAP
YYDS	85.54	99.30	99.78	81.64
w/o Texture-centered Relation	84.63 (-0.91)	98.81 (-0.49)	99.70 (-0.08)	81.43 (-0.21)
w/o Color-centered Relation	84.63 (-0.91)	98.53 (-0.77)	99.56 (-0.22)	81.23 (-0.41)
w/o Joint Relation	84.93 (-0.61)	98.99 (-0.31)	99.76 (-0.02)	80.50 (-1.14)

Table 5: Ablation study on different strategies of CMKR. For fair comparison, the best hyperparameters are selected for each strategy with grid-search.

Method	constrained	divided	extended	MA-LQE	SYSU		RegDB		LLCM	
					R-1	mAP	R-1	mAP	R-1	mAP
YYDS	-	-	-	-	85.54	81.64	90.16	83.52	58.22	65.09
+re-ranking [137]	-	-	-	-	95.24	93.19	92.18	91.82	72.63	76.61
	✓	-	-	-	93.37	90.07	95.98	94.84	70.93	74.75
	-	✓	-	-	95.40	93.23	96.73	94.47	73.39	77.13
	-	-	✓	-	95.40	93.72	96.51	96.79	73.01	77.25
	-	-	-	✓	95.51	93.77	96.65	96.13	73.41	77.35

datasets RegDB and LLCM. The results are shown in Tab.1 and Tab.2, and our methods outperform the other methods on all benchmarks by a large margin. On SYSU-MM01, YYDS achieves Rank1 85.54% and mAP 81.64% in the all-search mode, higher than STAR by 9.47% and 8.91%. CMKR further improves the performance to Rank1 95.51% and mAP 93.77%. On RegDB and LLCM, “YYDS+CMKR” achieves better scores than DEEN by 7.1% and 18.5% for Rank1, and 12.7% and 14.5% for mAP. This proves the effectiveness of our proposed network and re-ranking algorithm.

4.4 Ablation Study

YYDS. We conduct ablation studies of each component of YYDS in Tab.3. The introduction of color encoders improves the Rank1 and mAP by 11.30% and 10.66% respectively, which proves the complementarity of color information introduced by coarse descriptions. The text-IoU regularization is designed to alleviate the optimization confusion problem of color encoders, and achieves

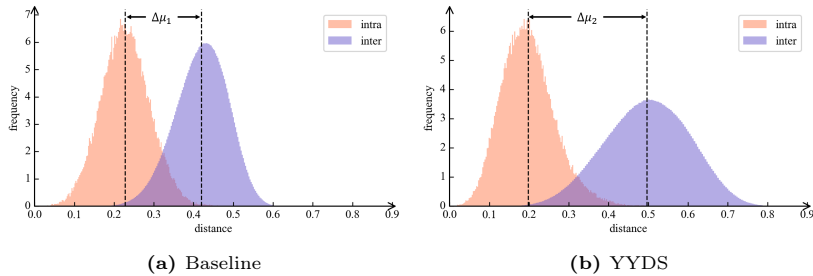


Fig. 6: The intra-identity and inter-identity distribution of feature distances of baseline and YYDS. (a) Baseline: $\Delta\mu_1 = 0.19$ (b) YYDS: $\Delta\mu_2 = 0.30$.

improvements of Rank1 0.88% and mAP 1.11%. Finally, the introduction of JRM further brings 1.00% gains in Rank1 and 1.63% gains in mAP. We further study the contributions of three relation modules $E_{j,t}^*$, $E_{j,c}^*$ and $E_{j,tc}^*$ in JRM in Tab.4. The results prove the effectiveness of the asymmetric design of JRM.

CMKR. We take k-reciprocal re-ranking [137] as baseline, and compare different neighbor strategies in Tab.5. The constrained strategy reduces performance on SYSU-MM01 and LLCM datasets, which is caused by losing intra-modal contextual information. Instead, both divided and extended strategies achieve consistent improvements on all three datasets, and the latter is taken as the default setting of our CMKR. Furthermore, MA-LQE solves the neighbor modality bias problem in neighbor features, and improves the Rank1 scores by 0.11%, 0.14% and 0.40% on three datasets.

Visualization Fig.6 visualize the feature distance distributions of baseline and YYDS on the SYSU-MM01 test set. We can observe that our method can widen the gap $\Delta\mu$ between the mean distances of intra-identity and inter-identity.

5 Conclusion

In this paper, we present a new task setting, named Refer-VI-ReID, to make up for the missing color information in infrared images with coarse descriptions. The main challenge lies in the misalignment between query modality and gallery modality. To solve this problem, we propose a Y-Y-shape decomposition structure (YYDS), which first decomposes the discriminative information into texture and color embeddings, and then aggregates them to the final features. Specially, an elaborately designed joint relation module is utilized to perform asymmetric relation and dynamic aggregation. While training, a text-IoU regularization strategy is introduced to solve the optimization confusion problem.

Considering that commonly used k-reciprocal re-ranking faces the neighbor modality bias problem in cross-modal scenarios, we thoroughly study three neighbor strategies and one query expansion strategy, and propose the cross-modal k-reciprocal re-ranking (CMKR) algorithm. Experimental results on SYSU-MM01, RegDB and LLCM prove the effectiveness of our proposed methods.

References

1. Bai, S., Bai, X.: Sparse contextual activation for efficient visual re-ranking. *IEEE Transactions on Image Processing* **25**(3), 1056–1069 (2016) [4](#)
2. Basaran, E., Gökmen, M., Kamasak, M.E.: An efficient framework for visible–infrared cross modality person re-identification. *Signal Processing: Image Communication* **87**, 115933 (2020) [4](#)
3. Bird, S., Klein, E., Loper, E.: Natural language processing with Python: analyzing text with the natural language toolkit. " O'Reilly Media, Inc." (2009) [8](#)
4. Chai, Z., Ling, Y., Luo, Z., Lin, D., Jiang, M., Li, S.: Dual-stream transformer with distribution alignment for visible-infrared person re-identification. *IEEE Transactions on Circuits and Systems for Video Technology* (2023) [11](#)
5. Chen, C., Ye, M., Qi, M., Wu, J., Jiang, J., Lin, C.W.: Structure-aware positional transformer for visible-infrared person re-identification. *IEEE Transactions on Image Processing* **31**, 2352–2364 (2022) [4](#)
6. Chen, X., Liu, X., Liu, W., Zhang, X.P., Zhang, Y., Mei, T.: Explainable person re-identification with attribute-guided metric distillation. In: *Proceedings of the IEEE/CVF International Conference on Computer Vision*. pp. 11813–11822 (2021) [2](#)
7. Chen, Y., Wan, L., Li, Z., Jing, Q., Sun, Z.: Neural feature search for rgb-infrared person re-identification. In: *Proceedings of the IEEE/CVF Conference on Computer Vision and Pattern Recognition*. pp. 587–597 (2021) [2](#), [4](#)
8. Chen, Y., Fan, Z., Chen, Z., Zhu, Y.: Ca-jaccard: Camera-aware jaccard distance for person re-identification. *arXiv preprint arXiv:2311.10605* (2023) [5](#)
9. Choi, S., Lee, S., Kim, Y., Kim, T., Kim, C.H.C.: Hierarchical cross-modality disentanglement for visible-infrared person re-identification. In: *Proceedings of the 2020 IEEE/CVF Conference Computer Vision Pattern Recognition, Seattle, WA, USA*. pp. 13–19 (2020) [2](#)
10. Choi, S., Lee, S., Kim, Y., Kim, T., Kim, C.: Hi-cmd: Hierarchical cross-modality disentanglement for visible-infrared person re-identification. In: *Proceedings of the IEEE/CVF conference on computer vision and pattern recognition*. pp. 10257–10266 (2020) [4](#)
11. Chollet, F.: Xception: Deep learning with depthwise separable convolutions. In: *Proceedings of the IEEE conference on computer vision and pattern recognition*. pp. 1251–1258 (2017) [7](#)
12. Chum, O., Philbin, J., Sivic, J., Isard, M., Zisserman, A.: Total recall: Automatic query expansion with a generative feature model for object retrieval. In: *2007 IEEE 11th International Conference on Computer Vision*. pp. 1–8. IEEE (2007) [9](#)
13. Chun, S., Oh, S.J., De Rezende, R.S., Kalantidis, Y., Larlus, D.: Probabilistic embeddings for cross-modal retrieval. In: *Proceedings of the IEEE/CVF Conference on Computer Vision and Pattern Recognition*. pp. 8415–8424 (2021) [2](#)
14. Dai, P., Ji, R., Wang, H., Wu, Q., Huang, Y.: Cross-modality person re-identification with generative adversarial training. In: *IJCAI*. vol. 1, p. 6 (2018) [2](#), [11](#)
15. Du, G., Zhang, L.: Enhanced invariant feature joint learning via modality-invariant neighbor relations for cross-modality person re-identification. *IEEE Transactions on Circuits and Systems for Video Technology* (2023) [4](#)
16. Du, Y., Lei, C., Zhao, Z., Dong, Y., Su, F.: Video-based visible-infrared person re-identification with auxiliary samples. *IEEE Transactions on Information Forensics and Security* **19**, 1313–1325 (2023) [2](#), [3](#)

17. Du, Y., Tong, Z., Wan, J., Zhang, B., Zhao, Y.: Pami-ad: An activity detector exploiting part-attention and motion information in surveillance videos. In: 2022 IEEE International Conference on Multimedia and Expo Workshops (ICMEW). pp. 1–6. IEEE (2022) [1](#)
18. Du, Y., Zhang, B., Ruan, X., Su, F., Zhao, Z., Chen, H.: Omg: Observe multiple granularities for natural language-based vehicle retrieval. In: Proceedings of the IEEE/CVF Conference on Computer Vision and Pattern Recognition. pp. 3124–3133 (2022) [2](#)
19. Du, Y., Zhao, Z., Song, Y., Zhao, Y., Su, F., Gong, T., Meng, H.: Strongsort: Make deepsort great again. *IEEE Transactions on Multimedia* (2023) [1](#)
20. Fan, X., Jiang, W., Luo, H., Mao, W.: Modality-transfer generative adversarial network and dual-level unified latent representation for visible thermal person re-identification. *The Visual Computer* pp. 1–16 (2022) [4](#)
21. Fang, X., Yang, Y., Fu, Y.: Visible-infrared person re-identification via semantic alignment and affinity inference. In: Proceedings of the IEEE/CVF International Conference on Computer Vision. pp. 11270–11279 (2023) [11](#)
22. Feng, J., Wu, A., Zheng, W.S.: Shape-erased feature learning for visible-infrared person re-identification. In: Proceedings of the IEEE/CVF Conference on Computer Vision and Pattern Recognition. pp. 22752–22761 (2023) [2, 4](#)
23. Fu, C., Hu, Y., Wu, X., Shi, H., Mei, T., He, R.: Cm-nas: Cross-modality neural architecture search for visible-infrared person re-identification. In: Proceedings of the IEEE/CVF International Conference on Computer Vision. pp. 11823–11832 (2021) [2, 4, 11](#)
24. Gao, C., Cai, G., Jiang, X., Zheng, F., Zhang, J., Gong, Y., Peng, P., Guo, X., Sun, X.: Contextual non-local alignment over full-scale representation for text-based person search. arXiv preprint arXiv:2101.03036 (2021) [3, 5, 10](#)
25. Garcia, J., Martinel, N., Micheloni, C., Gardel, A.: Person re-identification ranking optimisation by discriminant context information analysis. In: Proceedings of the IEEE International Conference on Computer Vision. pp. 1305–1313 (2015) [4](#)
26. Ge, Y., Li, Z., Zhao, H., Yin, G., Yi, S., Wang, X., et al.: Fd-gan: Pose-guided feature distilling gan for robust person re-identification. *Advances in neural information processing systems* **31** (2018) [2](#)
27. Goodfellow, I., Pouget-Abadie, J., Mirza, M., Xu, B., Warde-Farley, D., Ozair, S., Courville, A., Bengio, Y.: Generative adversarial nets. *Advances in neural information processing systems* **27** (2014) [2, 4](#)
28. Gordo, A., Almazan, J., Revaud, J., Larlus, D.: End-to-end learning of deep visual representations for image retrieval. *International Journal of Computer Vision* **124**(2), 237–254 (2017) [9](#)
29. Guo, R.P., Li, C.G., Li, Y., Lin, J.: Density-adaptive kernel based re-ranking for person re-identification. In: 2018 24th International Conference on Pattern Recognition (ICPR). pp. 982–987. IEEE (2018) [5](#)
30. Hao, X., Zhao, S., Ye, M., Shen, J.: Cross-modality person re-identification via modality confusion and center aggregation. In: Proceedings of the IEEE/CVF International conference on computer vision. pp. 16403–16412 (2021) [4, 6](#)
31. Hao, Y., Wang, N., Gao, X., Li, J., Wang, X.: Dual-alignment feature embedding for cross-modality person re-identification. In: Proceedings of the 27th ACM International Conference on Multimedia. pp. 57–65 (2019) [4](#)
32. Hao, Y., Wang, N., Li, J., Gao, X.: Hsme: Hypersphere manifold embedding for visible thermal person re-identification. In: Proceedings of the AAAI conference on artificial intelligence. vol. 33, pp. 8385–8392 (2019) [4](#)

33. He, K., Zhang, X., Ren, S., Sun, J.: Deep residual learning for image recognition. In: Proceedings of the IEEE conference on computer vision and pattern recognition. pp. 770–778 (2016) [6](#), [12](#)
34. He, L., Liao, X., Liu, W., Liu, X., Cheng, P., Mei, T.: Fastreid: A pytorch toolbox for general instance re-identification. In: Proceedings of the 31st ACM International Conference on Multimedia. pp. 9664–9667 (2023) [1](#)
35. He, S., Luo, H., Wang, P., Wang, F., Li, H., Jiang, W.: Transreid: Transformer-based object re-identification. In: Proceedings of the IEEE/CVF international conference on computer vision. pp. 15013–15022 (2021) [1](#)
36. Howard, A.G., Zhu, M., Chen, B., Kalenichenko, D., Wang, W., Weyand, T., Andreetto, M., Adam, H.: Mobilenets: Efficient convolutional neural networks for mobile vision applications. arXiv preprint arXiv:1704.04861 (2017) [7](#)
37. Hu, X., Zhou, Y.: Cross-modality person reid with maximum intra-class triplet loss. In: Pattern Recognition and Computer Vision: Third Chinese Conference, PRCV 2020, Nanjing, China, October 16–18, 2020, Proceedings, Part II 3. pp. 557–568. Springer (2020) [4](#)
38. Huang, S., Gong, B., Pan, Y., Jiang, J., Lv, Y., Li, Y., Wang, D.: Vop: Text-video co-operative prompt tuning for cross-modal retrieval. In: Proceedings of the IEEE/CVF Conference on Computer Vision and Pattern Recognition. pp. 6565–6574 (2023) [2](#)
39. Huang, Y., Wu, Q., Xu, J., Zhong, Y., Zhang, P., Zhang, Z.: Alleviating modality bias training for infrared-visible person re-identification. IEEE Transactions on Multimedia **24**, 1570–1582 (2021) [2](#), [4](#)
40. Huang, Z., Liu, J., Li, L., Zheng, K., Zha, Z.J.: Modality-adaptive mixup and invariant decomposition for rgb-infrared person re-identification. In: Proceedings of the AAAI Conference on Artificial Intelligence. vol. 36, pp. 1034–1042 (2022) [4](#)
41. Jambigi, C., Rawal, R., Chakraborty, A.: Mmd-reid: A simple but effective solution for visible-thermal person reid. arXiv preprint arXiv:2111.05059 (2021) [4](#)
42. Jegou, H., Harzallah, H., Schmid, C.: A contextual dissimilarity measure for accurate and efficient image search. In: 2007 IEEE Conference on computer vision and pattern recognition. pp. 1–8. IEEE (2007) [4](#)
43. Jegou, H., Schmid, C., Harzallah, H., Verbeek, J.: Accurate image search using the contextual dissimilarity measure. IEEE Transactions on Pattern Analysis and Machine Intelligence **32**(1), 2–11 (2008) [4](#)
44. Jia, M., Zhai, Y., Lu, S., Ma, S., Zhang, J.: A similarity inference metric for rgb-infrared cross-modality person re-identification. arXiv preprint arXiv:2007.01504 (2020) [3](#), [5](#), [10](#)
45. Jiang, D., Ye, M.: Cross-modal implicit relation reasoning and aligning for text-to-image person retrieval. In: Proceedings of the IEEE/CVF Conference on Computer Vision and Pattern Recognition. pp. 2787–2797 (2023) [2](#), [8](#)
46. Jiang, K., Zhang, T., Liu, X., Qian, B., Zhang, Y., Wu, F.: Cross-modality transformer for visible-infrared person re-identification. In: European Conference on Computer Vision. pp. 480–496. Springer (2022) [4](#)
47. Kalayeh, M.M., Basaran, E., Gökmen, M., Kamasak, M.E., Shah, M.: Human semantic parsing for person re-identification. In: Proceedings of the IEEE conference on computer vision and pattern recognition. pp. 1062–1071 (2018) [3](#)
48. Kim, M., Kim, S., Park, J., Park, S., Sohn, K.: Partmix: Regularization strategy to learn part discovery for visible-infrared person re-identification. In: Proceedings of the IEEE/CVF Conference on Computer Vision and Pattern Recognition. pp. 18621–18632 (2023) [4](#)

49. Kingma, D.P., Welling, M.: Auto-encoding variational bayes. arXiv preprint arXiv:1312.6114 (2013) [4](#)
50. Kong, J., He, Q., Jiang, M., Liu, T.: Dynamic center aggregation loss with mixed modality for visible-infrared person re-identification. *IEEE Signal Processing Letters* **28**, 2003–2007 (2021) [4](#)
51. Kramer, M.A.: Nonlinear principal component analysis using autoassociative neural networks. *AIChE journal* **37**(2), 233–243 (1991) [2](#), [4](#)
52. Leng, Q., Hu, R., Liang, C., Wang, Y., Chen, J.: Bidirectional ranking for person re-identification. In: 2013 IEEE International Conference on Multimedia and Expo (ICME). pp. 1–6. IEEE (2013) [4](#)
53. Leng, Q., Hu, R., Liang, C., Wang, Y., Chen, J.: Person re-identification with content and context re-ranking. *Multimedia Tools and Applications* **74**, 6989–7014 (2015) [4](#)
54. Li, D., Wei, X., Hong, X., Gong, Y.: Infrared-visible cross-modal person re-identification with an x modality. In: Proceedings of the AAAI conference on artificial intelligence. vol. 34, pp. 4610–4617 (2020) [4](#), [11](#)
55. Li, H., Liu, M., Hu, Z., Nie, F., Yu, Z.: Intermediary-guided bidirectional spatial-temporal aggregation network for video-based visible-infrared person re-identification. *IEEE Transactions on Circuits and Systems for Video Technology* (2023) [4](#)
56. Li, S., Xiao, T., Li, H., Zhou, B., Yue, D., Wang, X.: Person search with natural language description. In: Proceedings of the IEEE conference on computer vision and pattern recognition. pp. 1970–1979 (2017) [2](#)
57. Li, S., Sun, L., Li, Q.: Clip-reid: exploiting vision-language model for image re-identification without concrete text labels. In: Proceedings of the AAAI Conference on Artificial Intelligence. vol. 37, pp. 1405–1413 (2023) [1](#)
58. Li, W., Zhao, R., Xiao, T., Wang, X.: Deepreid: Deep filter pairing neural network for person re-identification. In: Proceedings of the IEEE conference on computer vision and pattern recognition. pp. 152–159 (2014) [1](#)
59. Li, X., Makihara, Y., Xu, C., Yagi, Y., Ren, M.: Gait recognition via semi-supervised disentangled representation learning to identity and covariate features. In: Proceedings of the IEEE/CVF Conference on Computer Vision and Pattern Recognition. pp. 13309–13319 (2020) [2](#)
60. Liang, W., Wang, G., Lai, J., Xie, X.: Homogeneous-to-heterogeneous: Unsupervised learning for rgb-infrared person re-identification. *IEEE Transactions on Image Processing* **30**, 6392–6407 (2021) [3](#), [5](#), [10](#)
61. Lin, X., Li, J., Ma, Z., Li, H., Li, S., Xu, K., Lu, G., Zhang, D.: Learning modal-invariant and temporal-memory for video-based visible-infrared person re-identification. In: Proceedings of the IEEE/CVF Conference on Computer Vision and Pattern Recognition. pp. 20973–20982 (2022) [2](#)
62. Ling, Y., Zhong, Z., Luo, Z., Rota, P., Li, S., Sebe, N.: Class-aware modality mix and center-guided metric learning for visible-thermal person re-identification. In: Proceedings of the 28th ACM international conference on multimedia. pp. 889–897 (2020) [4](#)
63. Liu, C., Chang, X., Shen, Y.D.: Unity style transfer for person re-identification. In: Proceedings of the IEEE/CVF conference on computer vision and pattern recognition. pp. 6887–6896 (2020) [3](#)
64. Liu, H., Tan, X., Zhou, X.: Parameter sharing exploration and hetero-center triplet loss for visible-thermal person re-identification. *IEEE Transactions on Multimedia* **23**, 4414–4425 (2020) [2](#), [4](#)

65. Liu, H., Ma, S., Xia, D., Li, S.: Sfanet: A spectrum-aware feature augmentation network for visible-infrared person reidentification. *IEEE Transactions on Neural Networks and Learning Systems* (2021) [4](#), [11](#)
66. Liu, Y., Ott, M., Goyal, N., Du, J., Joshi, M., Chen, D., Levy, O., Lewis, M., Zettlemoyer, L., Stoyanov, V.: Roberta: A robustly optimized bert pretraining approach. arXiv preprint arXiv:1907.11692 (2019) [6](#)
67. Lu, Z., Lin, R., Hu, H.: Tri-level modality-information disentanglement for visible-infrared person re-identification. *IEEE Transactions on Multimedia* (2023) [11](#)
68. Luo, C., Chen, Y., Wang, N., Zhang, Z.: Spectral feature transformation for person re-identification. In: *Proceedings of the IEEE/CVF international conference on computer vision*. pp. 4976–4985 (2019) [3](#)
69. Luo, H., Jiang, W., Gu, Y., Liu, F., Liao, X., Lai, S., Gu, J.: A strong baseline and batch normalization neck for deep person re-identification. *IEEE Transactions on Multimedia* **22**(10), 2597–2609 (2019) [1](#)
70. Luo, H., Ji, L., Zhong, M., Chen, Y., Lei, W., Duan, N., Li, T.: Clip4clip: An empirical study of clip for end to end video clip retrieval and captioning. *Neuro-computing* **508**, 293–304 (2022) [2](#)
71. Moon, H., Phillips, P.J.: Computational and performance aspects of pca-based face-recognition algorithms. *Perception* **30**(3), 303–321 (2001) [12](#)
72. Nguyen, D.T., Hong, H.G., Kim, K.W., Park, K.R.: Person recognition system based on a combination of body images from visible light and thermal cameras. *Sensors* **17**(3), 605 (2017) [12](#)
73. Niu, K., Huang, T., Huang, L., Wang, L., Zhang, Y.: Improving inconspicuous attributes modeling for person search by language. *IEEE transactions on image processing* (2023) [2](#)
74. Ouyang, J., Wu, H., Wang, M., Zhou, W., Li, H.: Contextual similarity aggregation with self-attention for visual re-ranking. *Advances in Neural Information Processing Systems* **34**, 3135–3148 (2021) [3](#)
75. Park, H., Lee, S., Lee, J., Ham, B.: Learning by aligning: Visible-infrared person re-identification using cross-modal correspondences. In: *Proceedings of the IEEE/CVF international conference on computer vision*. pp. 12046–12055 (2021) [4](#), [11](#)
76. Paszke, A., Gross, S., Massa, F., Lerer, A., Bradbury, J., Chanan, G., Killeen, T., Lin, Z., Gimelshein, N., Antiga, L., et al.: Pytorch: An imperative style, high-performance deep learning library. *Advances in neural information processing systems* **32** (2019) [12](#)
77. Peng, C., Wang, N., Li, J., Gao, X.: Re-ranking high-dimensional deep local representation for nir-vis face recognition. *IEEE Transactions on Image Processing* **28**(9), 4553–4565 (2019) [5](#)
78. Pu, N., Chen, W., Liu, Y., Bakker, E.M., Lew, M.S.: Dual gaussian-based variational subspace disentanglement for visible-infrared person re-identification. In: *Proceedings of the 28th ACM International Conference on Multimedia*. pp. 2149–2158 (2020) [4](#)
79. Qi, J., Liang, T., Liu, W., Li, Y., Jin, Y.: A generative-based image fusion strategy for visible-infrared person re-identification. *IEEE Transactions on Circuits and Systems for Video Technology* (2023) [4](#)
80. Qian, N.: On the momentum term in gradient descent learning algorithms. *Neural networks* **12**(1), 145–151 (1999) [12](#)
81. Qin, D., Gammeter, S., Bossard, L., Quack, T., Van Gool, L.: Hello neighbor: Accurate object retrieval with k-reciprocal nearest neighbors. In: *CVPR 2011*. pp. 777–784. *IEEE* (2011) [4](#)

82. Radenović, F., Tolias, G., Chum, O.: Fine-tuning cnn image retrieval with no human annotation. *IEEE transactions on pattern analysis and machine intelligence* **41**(7), 1655–1668 (2018) [9](#)
83. Russakovsky, O., Deng, J., Su, H., Krause, J., Satheesh, S., Ma, S., Huang, Z., Karpathy, A., Khosla, A., Bernstein, M., et al.: Imagenet large scale visual recognition challenge. *International journal of computer vision* **115**, 211–252 (2015) [12](#)
84. Sarfraz, M.S., Schumann, A., Eberle, A., Stiefelhagen, R.: A pose-sensitive embedding for person re-identification with expanded cross neighborhood re-ranking. In: *Proceedings of the IEEE conference on computer vision and pattern recognition*. pp. 420–429 (2018) [5](#)
85. Shao, Z., Zhang, X., Fang, M., Lin, Z., Wang, J., Ding, C.: Learning granularity-unified representations for text-to-image person re-identification. In: *Proceedings of the 30th ACM International Conference on Multimedia*. pp. 5566–5574 (2022) [2](#)
86. Shen, X., Xiao, Y., Hu, S.X., Sbai, O., Aubry, M.: Re-ranking for image retrieval and transductive few-shot classification. *Advances in Neural Information Processing Systems* **34**, 25932–25943 (2021) [3](#)
87. Sifre, L., Mallat, S.: Rigid-motion scattering for texture classification. *arXiv preprint arXiv:1403.1687* (2014) [7](#)
88. Sun, Y., Zheng, L., Yang, Y., Tian, Q., Wang, S.: Beyond part models: Person retrieval with refined part pooling (and a strong convolutional baseline). In: *Proceedings of the European conference on computer vision (ECCV)*. pp. 480–496 (2018) [1](#)
89. Tan, H., Liu, X., Bian, Y., Wang, H., Yin, B.: Incomplete descriptor mining with elastic loss for person re-identification. *IEEE Transactions on Circuits and Systems for Video Technology* **32**(1), 160–171 (2021) [3](#)
90. Wang, G.A., Zhang, T., Yang, Y., Cheng, J., Chang, J., Liang, X., Hou, Z.G.: Cross-modality paired-images generation for rgb-infrared person re-identification. In: *Proceedings of the AAAI conference on artificial intelligence*. vol. 34, pp. 12144–12151 (2020) [4](#), [11](#)
91. Wang, G., Zhang, T., Cheng, J., Liu, S., Yang, Y., Hou, Z.: Rgb-infrared cross-modality person re-identification via joint pixel and feature alignment. In: *Proceedings of the IEEE/CVF International Conference on Computer Vision*. pp. 3623–3632 (2019) [2](#), [4](#), [11](#)
92. Wang, H., Shen, J., Liu, Y., Gao, Y., Gavves, E.: Nformer: Robust person re-identification with neighbor transformer. In: *Proceedings of the IEEE/CVF Conference on Computer Vision and Pattern Recognition*. pp. 7297–7307 (2022) [3](#)
93. Wang, J., Zhang, Z., Chen, M., Zhang, Y., Wang, C., Sheng, B., Qu, Y., Xie, Y.: Optimal transport for label-efficient visible-infrared person re-identification. In: *Computer Vision–ECCV 2022: 17th European Conference, Tel Aviv, Israel, October 23–27, 2022, Proceedings, Part XXIV*. pp. 93–109. Springer (2022) [2](#)
94. Wang, Y., Wang, L., You, Y., Zou, X., Chen, V., Li, S., Huang, G., Hariharan, B., Weinberger, K.Q.: Resource aware person re-identification across multiple resolutions. In: *Proceedings of the IEEE conference on computer vision and pattern recognition*. pp. 8042–8051 (2018) [3](#)
95. Wang, Z., Fang, Z., Wang, J., Yang, Y.: Vitaa: Visual-textual attributes alignment in person search by natural language. In: *Computer Vision–ECCV 2020: 16th European Conference, Glasgow, UK, August 23–28, 2020, Proceedings, Part XII* 16. pp. 402–420. Springer (2020) [2](#)

96. Wang, Z., Gao, Z., Guo, K., Yang, Y., Wang, X., Shen, H.T.: Multilateral semantic relations modeling for image text retrieval. In: Proceedings of the IEEE/CVF Conference on Computer Vision and Pattern Recognition. pp. 2830–2839 (2023) [2](#)
97. Wang, Z., Wang, Z., Zheng, Y., Chuang, Y.Y., Satoh, S.: Learning to reduce dual-level discrepancy for infrared-visible person re-identification. In: Proceedings of the IEEE/CVF conference on computer vision and pattern recognition. pp. 618–626 (2019) [2](#)
98. Wei, X., Li, D., Hong, X., Ke, W., Gong, Y.: Co-attentive lifting for infrared-visible person re-identification. In: Proceedings of the 28th ACM international conference on multimedia. pp. 1028–1037 (2020) [4](#)
99. Wei, Z., Yang, X., Wang, N., Gao, X.: Syncretic modality collaborative learning for visible infrared person re-identification. In: Proceedings of the IEEE/CVF International Conference on Computer Vision. pp. 225–234 (2021) [4](#)
100. Wei, Z., Yang, X., Wang, N., Gao, X.: Dual-adversarial representation disentanglement for visible infrared person re-identification. *IEEE Transactions on Information Forensics and Security* (2023) [11](#)
101. Wu, A., Zheng, W.S., Yu, H.X., Gong, S., Lai, J.: Rgb-infrared cross-modality person re-identification. In: Proceedings of the IEEE international conference on computer vision. pp. 5380–5389 (2017) [2](#), [12](#)
102. Wu, J., Liu, H., Shi, W., Liu, M., Li, W.: Style-agnostic representation learning for visible-infrared person re-identification. *IEEE Transactions on Multimedia* (2023) [4](#), [11](#)
103. Wu, J., Liu, H., Su, Y., Shi, W., Tang, H.: Learning concordant attention via target-aware alignment for visible-infrared person re-identification. In: Proceedings of the IEEE/CVF International Conference on Computer Vision. pp. 11122–11131 (2023) [11](#)
104. Wu, Q., Dai, P., Chen, J., Lin, C.W., Wu, Y., Huang, F., Zhong, B., Ji, R.: Discover cross-modality nuances for visible-infrared person re-identification. In: Proceedings of the IEEE/CVF Conference on Computer Vision and Pattern Recognition. pp. 4330–4339 (2021) [11](#)
105. Yan, S., Dong, N., Zhang, L., Tang, J.: Clip-driven fine-grained text-image person re-identification. *IEEE Transactions on Image Processing* (2023) [2](#)
106. Yang, F., Wang, Z., Xiao, J., Satoh, S.: Mining on heterogeneous manifolds for zero-shot cross-modal image retrieval. In: Proceedings of the AAAI Conference on Artificial Intelligence. vol. 34, pp. 12589–12596 (2020) [11](#)
107. Yang, M., Huang, Z., Hu, P., Li, T., Lv, J., Peng, X.: Learning with twin noisy labels for visible-infrared person re-identification. In: Proceedings of the IEEE/CVF conference on computer vision and pattern recognition. pp. 14308–14317 (2022) [11](#)
108. Ye, H., Liu, H., Meng, F., Li, X.: Bi-directional exponential angular triplet loss for rgb-infrared person re-identification. *IEEE Transactions on Image Processing* **30**, 1583–1595 (2020) [4](#)
109. Ye, M., Chen, J., Leng, Q., Liang, C., Wang, Z., Sun, K.: Coupled-view based ranking optimization for person re-identification. In: *MultiMedia Modeling: 21st International Conference, MMM 2015, Sydney, NSW, Australia, January 5-7, 2015, Proceedings, Part I* 21. pp. 105–117. Springer (2015) [4](#)
110. Ye, M., Lan, X., Leng, Q.: Modality-aware collaborative learning for visible thermal person re-identification. In: Proceedings of the 27th ACM International Conference on Multimedia. pp. 347–355 (2019) [4](#), [6](#)

111. Ye, M., Lan, X., Leng, Q., Shen, J.: Cross-modality person re-identification via modality-aware collaborative ensemble learning. *IEEE Transactions on Image Processing* **29**, 9387–9399 (2020) [2](#)
112. Ye, M., Lan, X., Li, J., Yuen, P.: Hierarchical discriminative learning for visible thermal person re-identification. In: *Proceedings of the AAAI Conference on Artificial Intelligence*. vol. 32 (2018) [2](#), [4](#)
113. Ye, M., Lan, X., Wang, Z., Yuen, P.C.: Bi-directional center-constrained top-ranking for visible thermal person re-identification. *IEEE Transactions on Information Forensics and Security* **15**, 407–419 (2019) [2](#), [4](#)
114. Ye, M., Liang, C., Yu, Y., Wang, Z., Leng, Q., Xiao, C., Chen, J., Hu, R.: Person reidentification via ranking aggregation of similarity pulling and dissimilarity pushing. *IEEE Transactions on Multimedia* **18**(12), 2553–2566 (2016) [4](#)
115. Ye, M., Ruan, W., Du, B., Shou, M.Z.: Channel augmented joint learning for visible-infrared recognition. In: *Proceedings of the IEEE/CVF International Conference on Computer Vision*. pp. 13567–13576 (2021) [4](#), [11](#)
116. Ye, M., Shen, J., J. Crandall, D., Shao, L., Luo, J.: Dynamic dual-attentive aggregation learning for visible-infrared person re-identification. In: *Computer Vision—ECCV 2020: 16th European Conference, Glasgow, UK, August 23–28, 2020, Proceedings, Part XVII 16*. pp. 229–247. Springer (2020) [2](#), [11](#), [12](#)
117. Ye, M., Shen, J., Lin, G., Xiang, T., Shao, L., Hoi, S.C.: Deep learning for person re-identification: A survey and outlook. *IEEE transactions on pattern analysis and machine intelligence* **44**(6), 2872–2893 (2021) [1](#), [11](#)
118. Ye, M., Shen, J., Shao, L.: Visible-infrared person re-identification via homogeneous augmented tri-modal learning. *IEEE Transactions on Information Forensics and Security* **16**, 728–739 (2020) [4](#)
119. Ye, M., Wang, Z., Lan, X., Yuen, P.C.: Visible thermal person re-identification via dual-constrained top-ranking. In: *IJCAI*. vol. 1, p. 2 (2018) [2](#), [4](#)
120. Yu, H., Cheng, X., Peng, W., Liu, W., Zhao, G.: Modality unifying network for visible-infrared person re-identification. In: *Proceedings of the IEEE/CVF International Conference on Computer Vision*. pp. 11185–11195 (2023) [4](#), [11](#)
121. Yu, R., Zhou, Z., Bai, S., Bai, X.: Divide and fuse: A re-ranking approach for person re-identification. *arXiv preprint arXiv:1708.04169* (2017) [5](#)
122. Zhang, G., Zhang, Y., Tan, Z.: Protohpe: Prototype-guided high-frequency patch enhancement for visible-infrared person re-identification. In: *Proceedings of the 31st ACM International Conference on Multimedia*. pp. 944–954 (2023) [4](#)
123. Zhang, Q., Lai, C., Liu, J., Huang, N., Han, J.: Fmcnet: Feature-level modality compensation for visible-infrared person re-identification. In: *Proceedings of the IEEE/CVF Conference on Computer Vision and Pattern Recognition*. pp. 7349–7358 (2022) [4](#)
124. Zhang, S., Chen, C., Song, W., Gan, Z.: Deep feature learning with attributes for cross-modality person re-identification. *Journal of Electronic Imaging* **29**(3), 033017–033017 (2020) [4](#)
125. Zhang, Y., Lu, H.: Deep cross-modal projection learning for image-text matching. In: *Proceedings of the European conference on computer vision (ECCV)*. pp. 686–701 (2018) [2](#), [8](#)
126. Zhang, Y., Zhao, S., Kang, Y., Shen, J.: Modality synergy complement learning with cascaded aggregation for visible-infrared person re-identification. In: *European Conference on Computer Vision*. pp. 462–479. Springer (2022) [2](#), [4](#), [11](#)
127. Zhang, Y., Wang, H.: Diverse embedding expansion network and low-light cross-modality benchmark for visible-infrared person re-identification. In: *Proceedings*

- of the IEEE/CVF Conference on Computer Vision and Pattern Recognition. pp. 2153–2162 (2023) [8](#), [11](#), [12](#)
128. Zhang, Y., Yan, Y., Lu, Y., Wang, H.: Towards a unified middle modality learning for visible-infrared person re-identification. In: Proceedings of the 29th ACM International Conference on Multimedia. pp. 788–796 (2021) [4](#), [11](#)
 129. Zhang, Y., Qian, Q., Wang, H., Liu, C., Chen, W., Wan, F.: Graph convolution based efficient re-ranking for visual retrieval. *IEEE Transactions on Multimedia* (2023) [3](#)
 130. Zhang, Z., Tran, L., Yin, X., Atoum, Y., Liu, X., Wan, J., Wang, N.: Gait recognition via disentangled representation learning. In: Proceedings of the IEEE/CVF conference on computer vision and pattern recognition. pp. 4710–4719 (2019) [2](#)
 131. Zhang, Z., Jiang, S., Huang, C., Li, Y., Da Xu, R.Y.: Rgb-ir cross-modality person reid based on teacher-student gan model. *Pattern Recognition Letters* **150**, 155–161 (2021) [4](#)
 132. Zheng, A., Pan, P., Li, H., Li, C., Luo, B., Tan, C., Jia, R.: Progressive attribute embedding for accurate cross-modality person re-id. In: Proceedings of the 30th ACM International Conference on Multimedia. pp. 4309–4317 (2022) [4](#), [11](#)
 133. Zheng, L., Zhang, H., Sun, S., Chandraker, M., Yang, Y., Tian, Q.: Person re-identification in the wild. In: Proceedings of the IEEE conference on computer vision and pattern recognition. pp. 1367–1376 (2017) [1](#)
 134. Zheng, Z., Yang, X., Yu, Z., Zheng, L., Yang, Y., Kautz, J.: Joint discriminative and generative learning for person re-identification. In: proceedings of the IEEE/CVF conference on computer vision and pattern recognition. pp. 2138–2147 (2019) [2](#)
 135. Zheng, Z., Zheng, L., Garrett, M., Yang, Y., Xu, M., Shen, Y.D.: Dual-path convolutional image-text embeddings with instance loss. *ACM Transactions on Multimedia Computing, Communications, and Applications (TOMM)* **16**(2), 1–23 (2020) [2](#)
 136. Zhong, X., Lu, T., Huang, W., Ye, M., Jia, X., Lin, C.W.: Grayscale enhancement colorization network for visible-infrared person re-identification. *IEEE Transactions on Circuits and Systems for Video Technology* **32**(3), 1418–1430 (2021) [2](#)
 137. Zhong, Z., Zheng, L., Cao, D., Li, S.: Re-ranking person re-identification with k-reciprocal encoding. In: Proceedings of the IEEE conference on computer vision and pattern recognition. pp. 1318–1327 (2017) [3](#), [4](#), [9](#), [13](#), [14](#)
 138. Zhong, Z., Zheng, L., Kang, G., Li, S., Yang, Y.: Random erasing data augmentation. In: Proceedings of the AAAI conference on artificial intelligence. vol. 34, pp. 13001–13008 (2020) [12](#)
 139. Zhong, Z., Zheng, L., Zheng, Z., Li, S., Yang, Y.: Camera style adaptation for person re-identification. In: Proceedings of the IEEE conference on computer vision and pattern recognition. pp. 5157–5166 (2018) [1](#)
 140. Zhou, K., Yang, Y., Cavallaro, A., Xiang, T.: Learning generalisable omni-scale representations for person re-identification. *IEEE transactions on pattern analysis and machine intelligence* **44**(9), 5056–5069 (2021) [1](#)
 141. Zhu, Y., Yang, Z., Wang, L., Zhao, S., Hu, X., Tao, D.: Hetero-center loss for cross-modality person re-identification. *Neurocomputing* **386**, 97–109 (2020) [4](#)